Nephrol Dial Transplant (2018) 33: ii41–ii50
doi: 10.1093/ndt/gfy198

ndt
Nephrology Dialysis Transplantation

REVIEW

Magnetic resonance imaging T_1- and T_2-mapping to assess renal structure and function: a systematic review and statement paper

Marcos Wolf[1], Anneloes de Boer[2], Kanishka Sharma[3], Peter Boor[4], Tim Leiner[5], Gere Sunder-Plassmann[6], Ewald Moser[7], Anna Caroli[8] and Neil Peter Jerome[9,10]

[1]Center for Medical Physics and Biomedical Engineering, MR-Centre of Excellence, Medical University of Vienna, Vienna, Austria, [2]Department of Radiology, University Medical Center Utrecht, Utrecht University, Utrecht, The Netherlands, [3]Biomedical Imaging Science Department, Leeds Institute of Cardiovascular and Metabolic Medicine, University of Leeds, Leeds, UK, [4]Institute of Pathology & Division of Nephrology, RWTH University of Aachen, Aachen, Germany, [5]Department of Radiology, University Medical Center Utrecht, Utrecht University, Utrecht, The Netherlands, [6]Department of Medicine III, Division of Nephrology and Dialysis, General Hospital and Medical University of Vienna, Vienna, Austria, [7]Center for Medical Physics and Biomedical Engineering, MR-Centre of Excellence, Medical University of Vienna, Vienna, Austria, [8]Medical Imaging Unit, Bioengineering Department, IRCCS Istituto di Ricerche Farmacologiche Mario Negri, Bergamo, Italy, [9]Clinic of Radiology and Nuclear Medicine, St. Olavs University Hospital, Trondheim, Norway and [10]Department of Circulation and Medical Imaging, NTNU – Norwegian University of Science and Technology, Trondheim, Norway

Correspondence and offprint requests to: Marcos Wolf; E-mail: marcos.wolf@meduniwien.ac.at; Twitter handle: @renalMRI

ABSTRACT

This systematic review, initiated by the European Cooperation in Science and Technology Action Magnetic Resonance Imaging Biomarkers for Chronic Kidney Disease (PARENCHIMA), focuses on potential clinical applications of magnetic resonance imaging in renal non-tumour disease using magnetic resonance relaxometry (MRR), specifically, the measurement of the independent quantitative magnetic resonance relaxation times T_1 and T_2 at 1.5 and 3Tesla (T), respectively. Healthy subjects show a distinguishable cortico-medullary differentiation (CMD) in T_1 and a slight CMD in T_2. Increased cortical T_1 values, that is, reduced T_1 CMD, were reported in acute allograft rejection (AAR) and diminished T_1 CMD in chronic allograft rejection. However, ambiguous findings were reported and AAR could not be sufficiently differentiated from acute tubular necrosis and cyclosporine nephrotoxicity. Despite this, one recent quantitative study showed in renal transplants a direct correlation between fibrosis and T_1 CMD. Additionally, various renal diseases, including renal transplants, showed a moderate to strong correlation between T_1 CMD and renal function. Recent T_2 studies observed increased values in renal transplants compared with healthy subjects and in early-stage autosomal dominant polycystic kidney disease (ADPKD), which could improve diagnosis and progression assessment compared with total kidney volume alone in early-stage ADPKD. Renal MRR is suggested to be sensitive to renal perfusion, ischaemia/oxygenation, oedema, fibrosis, hydration and comorbidities, which reduce specificity. Due to the lack of standardization in patient preparation, acquisition protocols and adequate patient selection, no widely accepted reference values are currently available. Therefore this review encourages efforts to optimize and standardize (multi-parametric) protocols to increase specificity and to tap the full potential of renal MRR in future research.

Keywords: magnetic resonance imaging, kidney, mapping, relaxometry, chronic kidney disease

INTRODUCTION

Kidneys are morphologically complex organs. Renal pathologies induce (micro-) structural and functional changes that may be captured with magnetic resonance imaging (MRI) owing to its exceptional soft tissue contrast. Despite the frequent and successful use of magnetic resonance relaxometry (MRR) in other organs (e.g. cardiac MRI) to assess oedema, amyloid deposition and fibrosis, the application of renal MRR is still scarce.

Renal MRR holds the promise to non-invasively quantify tissue inflammation and alterations, such as interstitial or cellular oedema and/or fibrosis, as well as renal function. This review article evaluates and summarizes data on renal T_1 and T_2 mapping using clinical 1.5 and 3Tesla (T) systems and provides

recommendations for upcoming research efforts to promote MRR in clinical practice.

MATERIALS AND METHODS

The European Cooperation in Science and Technology (COST) Action Magnetic Resonance Imaging Biomarkers for Chronic Kidney Disease (PARENCHIMA) (www.renalmri.org) initiated this systematic review by an extended PubMed search regarding renal mapping (see Supplementary data) on 25 October 2017 to identify human *in vivo* T_1 and T_2 measurements at 1.5 and 3T. Titles and abstracts of 357 publications were processed to identify matches aligning with the aim of this article. Furthermore, relevant references within the acquired papers and selected studies by the authors were added. Our analysis reaches back to the year 1983 and includes studies with field strengths below 1.5T. Some handpicked qualitative studies and preclinical studies were also included to present readers with relevant trends in the measurement of renal T_1 and T_2 values. Studies regarding renal neoplasms and/or dynamic contrast-enhanced MRI were excluded. For details on data collection, see Supplementary data.

BASIC PRINCIPLES OF MAGNETIC RELAXATION MECHANISMS

MRI is a non-invasive technique to map the human body using the interaction of three magnetic fields: (i) a strong static field (B_0 or main magnet) to magnetize the whole sample and to allow the signal to be measured; (ii) gradient coils producing three ($G_{x, y, z}$) linear, orthogonal gradients to allow the signal to be registered in space; and (iii) a dynamic radio frequency (RF) field (B_1 or excitation field) to change steady-state magnetization produced by B_0 and to enable the readout of the measured signal (using an appropriately frequency-tuned coil or antenna) [1].

When subjects are placed inside the MRI scanner, nuclear spins align with B_0 (Figure 1a and b). The application of an RF pulse (B_1; usually in the range of milliseconds and millitesla) changes this macroscopic magnetization and proton spins are perturbed (i.e. tipped away from B_0). RF pulses are named after their effect on the net magnetization vector, i.e. an RF pulse tilting the net magnetization vector by 90° from the *z* direction (B_0) into the *x*/*y* plane is called a 90° pulse and a 180° pulse inverts the magnetization vector (i.e. z to −z; Figure 1a and b). The return of the tipped net magnetic vector to the steady-state equilibrium along the B_0 axis and the decay of net transverse magnetization, respectively, are two independent processes that can be measured [2]; namely spin–lattice (T_1) and spin–spin (T_2) relaxation time. T_1 and T_2 relaxation times are characteristic for the tissue composition (i.e. local microstructural magnetochemical environment) and provide the main sources of tissue contrast in morphological MRI.

In order to actually quantify T_1 or T_2 relaxation times (i.e. T_1 and T_2 mapping) different clinical MRI protocols are available with specific advantages and disadvantages; the chosen method is often determined by the available MRI hardware, sequence and acquisition time. However, over the years, a plethora of measurement sequences and acronyms have been published, and the interested reader should refer to an in-depth textbook written particularly for medical doctors [3].

T_1 relaxation time

The gold standard for T_1 measurement, the inversion recovery (IR) technique, first inverts the magnetization in the *z* direction using a 180° pulse, which is followed by a waiting time, TI (inversion time), and a successive 90° pulse to initiate data readout with further 180° pulses. This IR preparation module has to be repeated several times by incrementing TI to acquire three to eight data points using a long TR (repetition time; i.e. five to seven times T_1), to ensure full relaxation before each inversion pulse, which leads to long overall IR-T_1 measurement times (Figure 1a and c).

The desire for faster T_1 measurement compatible with individual breath-holds has given rise to several efficient methods, the most common being variable flip-angle (VFA) and modified Look-Locker imaging (MOLLI).

In VFA, two or more spoiled gradient recalled-echo acquisitions with differing excitation pulse flip-angles give rise to signals modulated by T_1 [4]; while substantially faster than IR-T_1, care must be taken before considering VFA to provide quantitative, rather than relative, T_1 measures [5]. VFA measurements are susceptible to B_1 inhomogeneity and thus require additional B_1 mapping. Also, the accuracy of the resulting T_1 depends on the relation of the chosen flip-angles with respect to the observed T_1 range.

The MOLLI sequence and its variants, based on the technique developed in 1970 by Look and Locker [6], sacrifice the requirement of pre-excitation equilibrium to save time and report a modified, shorter, apparent T_1 (often denoted T_1*) derived from repeated efficient sampling of a single excitation pulse. This type of sequence is sufficiently fast, so it is well suited for cardiac imaging, but the comparability between T_1 and T_1* is limited [7, 8].

T_2 relaxation time

The most common method to measure T_2 relaxation time is a multi-echo (fast) spin-echo sequence, which first applies a 90° pulse to tilt the magnetization into the *x*/*y* plane and then applies several 180° pulses in the *x*/*y* plane to recover (echo) magnetization and hence enables T_2 estimates from the signal envelope (Figure 1b and d). This approach is achieved within one TR, which is much faster than T_1 (IR) measurements, and allows full kidney coverage within a few breath-holds.

However, T_2 measurements are sensitive to imperfect slice selection pulse profiles, diffusion, flow and field inhomogeneities [9]. A T_2 preparation module decreases the influence of imperfect slice selection profiles, diffusion and flow. Carr–Purcell–Meiboom–Gill (CPMG) and similar preparations can help to compensate for field inhomogeneities. Therefore T_2 preparations yield more accurate (but slightly higher) T_2 values as compared with a multi-echo spin-echo approach. T_2 preparations are widely used in cardiac imaging to visualize oedema after myocardial infarction [10], and can be performed during free breathing, although image registration prior to T_2 calculation is required. Commonly at least three source images with

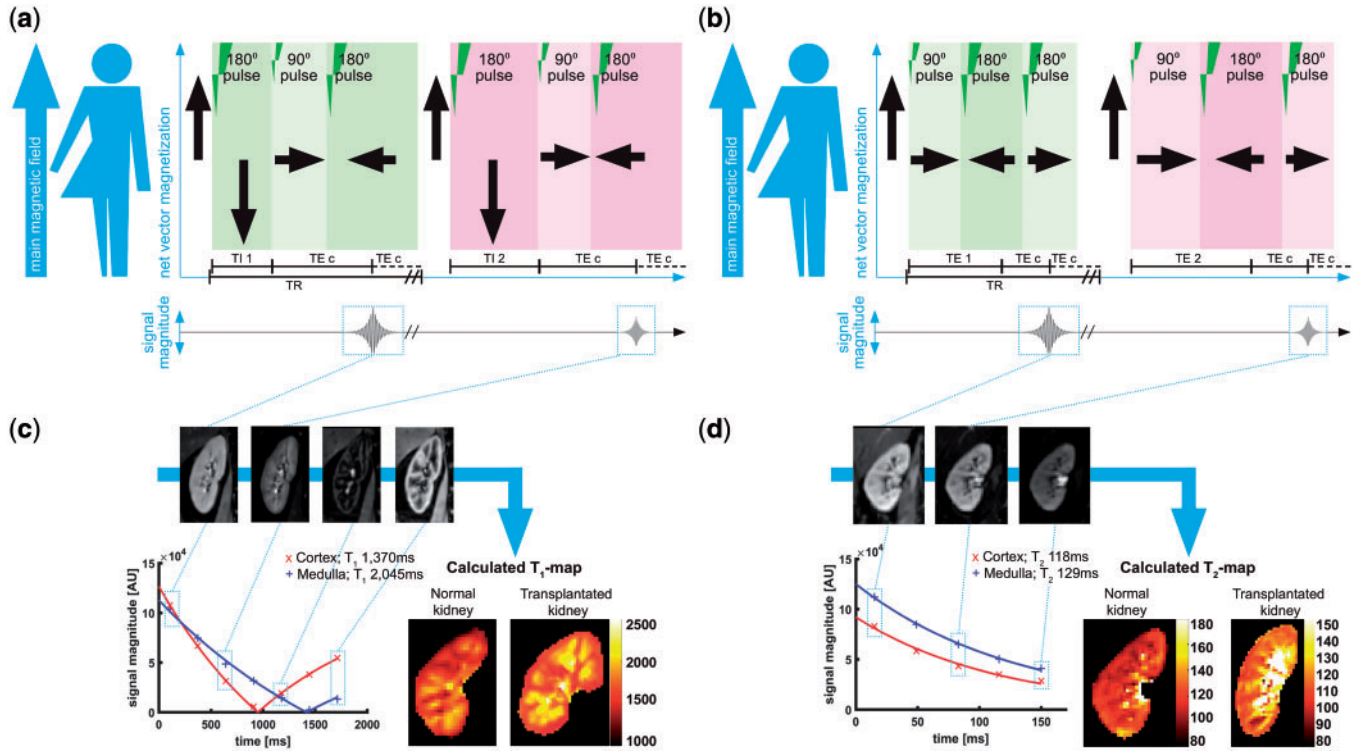

FIGURE 1: Simplified illustration of the quantification of T_1 (a, c), and T_2 (b, d) relaxation time measurements in the cortex (red) and medulla (blue). The illustration on the left (a, b) shows the patient lying inside the MRI scanner (view from above). The main magnetic field (B_0) is in the foot–head direction. The static magnetic field causes some nuclear spins to align parallel with B_0, which is illustrated with the first big black arrow in the graphic next to it. (**a**) Simplified sequence diagram for T_1 mapping. The gold standard for T_1 relaxation time measurements is initiated by a 180° pulse (IR). As a consequence, the net magnetization is tilted in the *z* direction (from left to right; first grey arrow). Thereafter a waiting time is applied, TI 1 (time of inversion), which ends after the application of a 90° pulse, so that the net magnetization is tilted in the *x*/*y* plane and the readout with constant time of echo (TE c) begins. After a long time of repetition (TR) the next measurement begins; however, the waiting time is longer (TI 2). The graphic below shows the acquired signal, which shows a stronger signal for the first measurement and a weaker signal for the second measurement (see dashes boxes). (**b**) Simplified sequence diagram for T_2 mapping. The most commonly used protocol is initiated by a 90° pulse and a 180° pulse, which tilts the net magnetization first into the *x*/*y* plane and thereafter into the opposite direction. This process is differently timed (TE 1 and TE 2). After successive 180° pulses the readout begins with TE c. Below, the acquired signal is shown. Notice the exemplified and reduced signal magnitude of the second signal (dashed boxes). (**c**) Multiple inversion time acquisitions for T_1 mapping. On the bottom left, the graph shows the measured signal magnitude for each inversion time of the IR sequence. Due to the IR the T_1 signal decays first towards null and recovers afterwards, which can also be depicted in the corresponding images of the native kidney on the top left. The T_1 signal decay curve is used to calculate a color-coded T_1 map (examples of normal and transplanted kidney; colour bar in ms). (**d**) The graph on the bottom left shows the T_2 signal decay during the multiple echo time acquisition for the T_2 mapping data. Corresponding images of the native kidney is shown on the top left. The T_2 signal decay curve is used to calculate a colour-coded T_2 map (examples of normal and transplanted kidney; colour bar in ms). Figure layout, design, and editing: Karin van Rijnbach, A.d.B., N.P.J. and M.W.; image data acquisition and reconstruction: A.d.B.

different echo times are recommended for accurate T_2 estimation using two- or three-parameter exponential fittings [10–13].

RENAL T_1 MAPPING

Reference values and physiological modulations

In the early 1980s, renal MRI detected relatively increased T_1 values in the medulla compared with the cortex in healthy subjects. This corticomedullary differentiation (CMD) is presumably caused by the higher free water content, i.e. higher mobility of water molecules, in the medullary tubules and collecting ducts [14, 15]. Additionally Hricak *et al.* [14] reported that hydration and the water balance management of the kidneys are important influencing factors, because T_1 CMD decreases during dehydration (relative cortical T_1 increase) and increases after rehydration, i.e. forced diuresis [14], but the impact in healthy subjects or patients was never reassessed at 1.5 T and 3T. Another inevitable variation is caused by the increase of B_0 from 1.5 and 3T, as T_1 generally increases. Further variation of renal T_1 values was reported due to different MRI acquisition schemes and breathing strategies [16, 17], even though high interexamination repeatability for single acquisition schemes was proven [18–20]. Therefore no widely accepted reference values are published and the given limitations have to be considered when comparing different studies (Table 1).

T_1 modulation by the inhalation of oxygen and carbogen. T_1 and T_2* relaxation times are modulated by oxygen level changes in the blood and/or tissue, although caused by different mechanisms [21]. T_2*, i.e. blood oxygen level

Table 1. Quantitative T_1 studies at 1.5 and 3T

Author	Year	Subject	Sample size	Group	*In vivo* repeatability	GFR	Hydration	Respiratory compensation	Sequence	Cortex	Medulla	Other modalities
1.5T												
Blüml *et al.* [16]	1993	Healthy	9	—	No	Not measured	None	BH	IR TurboFLASH	966 ± 41	1320 ± 76	–
Jones *et al.* [21]	2002	Healthy	9	Normoxia	No	Not measured	None	BH	IR segmented half Fourier TSE	882 ± 59*	1163 ± 118	–
			9	Pure O_2						829 ± 70*	1159 ± 117	
de Bazelaire *et al.* [11]	2004	Healthy	4	—	No	Not measured	None	BH	IR SS FSE, half Fourier	996 ± 58	1412 ± 58	T_2
Lee *et al.* [22]	2007	Underlying renal disease unknown	10	Mixed: 1 patient with CKD and hypertension; 9 patients with only hypertension; 3 patients had RAS	No	mGFR: SKGFR^{99m} Tc-DTPA	No fasting. Subjects drank ∼300mL prior the MR acquisition and voided	BH	IR trueFISP	1083 ± 149	1229 ± 118	–
O'Connor *et al.* [23]	2007	Healthy	5	Normoxia (21% O_2)	No	Not measured	None	FB	VFA 3D T1w FFE	945 ± 15◀,▼	Not measured	–
			5	Pure O_2						883 ± 9◀		
			5	Carbongen (95% O_2 & 5% CO_2)						873 ± 22▼		
O'Connor *et al.* [24]	2009	Healthy	6	Normoxia (21% O_2)	No	Not measured	4-h fasting	FB	VFA 3D RF-spoiled T1w FFE	961 ± 48∫,§	Not measured	T_2*
			6	Pure O_2						897 ± 27∫		
			6	Carbongen (95% O_2 & 5% CO_2)						909 ± 35§		
Huang *et al.* [19]	2011	Underlying renal disease unknown	5	Native kidney; eGFR <60 (32 ±13)	Yes	MDRD eGFR	4-h fasting	BH	IR SS FSE	1145 ± 216[a]	1392 ± 110[a]	–
			7	Native kidney; eGFR >60 (80 ±7)						995 ± 216[a] 1057 ± 94•	1387 ± 119[a] 1389 ± 48◇	
		Renal allograft	11	eGFR <60 (42 ±15)						1231 ± 191[a]	1621 ±190[a]	
			4	eGFR >60 (73 ±5)						1051 ± 179[a] 1183 ±136•	1439 ±113[a] 1573 ± 132◇	
Breidthardt *et al.* [25]	2015	Young healthy	10	Mean eGFR 101 ±17	No	MDRD eGFR	None	TRIG	IR bFFE	1080 ± 68	Not measured	ASL
		Healthy	10	Age-matched volunteers; mean eGFR 75 ±16						1030 ± 55 1054 ± 65■		
		Preserved renal function	10	cHF: mean eGFR 73 ±8	No	MDRD eGFR	None	TRIG	IR bFFE	1067 ± 79□	Not measured	ASL
		Impaired renal funciton	10	cHF: mean eGFR 38 ±11						1169 ± 100□ 1121 ± 102■		
Chen *et al.* [17]	2016	Healthy	9	—	No	Not measured	None	BH	MOLLI	827 ± 50	1381 ± 95	–
Cox *et al.* [18]	2017	Healthy	8	—	No	eGFR	2-h fasting	BH	IR SE EPI	1024 ± 71	1272 ± 140	–
			58						bFFE	1053 ± 72	–	
			38							–	1318 ± 98	

Peperhove *et al.* [26]	2018	Healthy	14	Native kidneys	No	Cockroft–Gault eGFR	None	BH	MOLLI	987 ± 102$^{\blacktriangleleft}$	1428 ± 98$^{\#}$	–
		LuTx	52	Native kidneys						1058 ± 96$^{\blacktriangledown}$	1414 ± 101$^{\blacktriangleright}$	
		Renal allograft	49	Renal allograft						1299 ± 101$^{\blacktriangledown,\blacktriangleleft}$	1516 ± 76$^{\blacktriangleright,\#}$	
		Healthy, LuTx and renal allograpft mixed	47	eGFR ≥90						1058 ± 108	1427 ± 89†	
			26	eGFR 60–89	No	Cockroft–Gault eGFR	None	BH	MOLLI	1077 ± 132 ‡	1421 ± 123°	–
			16	eGFR 30–59						1273 ± 97	1541 ± 51$^{\dagger,\circ}$	
			18	eGFR 15–29						1297 ± 113 ‡	1497 ± 97	
			8	eGFR <15						1377 ± 109	1515 ± 45	
3T												
de Bazelaire *et al.* [11]	2004	Healthy	6	—	No	Not measured	None	BH	IR SS FSE, half-Fourier	1142 ± 154	1545 ± 142	T_2
Ding *et al.* [27]	2013	Healthy	7	Normoxia; conventional acquisition	No	Not measured	None	BH	IR HASTE breath	1187 ± 112	1523 ± 116	T_2*
			7	Normoxia; novel acquisition				TRIG	MS ME GE EPI interleaved with MS IR EPI	1240 ± 130	1567 ± 121	
			7	Pure O_2; novel acquisition						1171 ± 212	1578 ± 123	
Gillis *et al.* [20]	2014	Healthy	12	MRI 1; eGFR 98 ± 15	Yes	CKD eGFR	6-h fasting	BH	MOLLI	1376 ± 104	1651 ± 86	–
				MRI 2; eGFR 98 ± 15						1406 ± 96	1639 ± 80	
Li *et al.* [12]	2015	Healthy	5	—	No	No	None	BH	IR SS FSE	1261 ± 86	1676 ± 94	T_2
Chen *et al.* [17]	2016	Healthy	26	—	No	No	None	BH	MOLLI	1194 ± 88	1610 ± 55	–
Gillis *et al.* [28]	2016	Healthy	24	Mean eGFR 100 ± 14	No	CKD-EPI eGFR	None	BH	MOLLI	1366 ± 122$^{\blacktriangleleft}$	Not measured	–
		CKD	17	Mean eGFR 40 ± 25	No	CKD-EPI eGFR	None	BH	MOLLI	1550 ± 81$^{\blacktriangleleft}$	Not measured	–
Friedli *et al.* [29]	2016	Renal allograft	29	Renal allograft	No	CKD-EPI eGFR	None	BH	MOLLI	1334 ± 57	1473 ± 48	–
Cox *et al.* [18]	2017	Healthy	21	—	Yes	Not measured	2-h fasting	TRIG	IR SE EPI	1367 ± 79	–	T_2*, DWI, PC, ASL
		Healthy	20							–	1655 ± 76	
		Healthy	26						IR bFFE	1124 ± 114	–	
		Healthy	25							–	1388 ± 126	
		Healthy	13	Age < 40 a					IR SE EPI	1347 ± 65	–	
		Healthy	12	Age < 40 a						–	1635 ± 66	
		Healthy	8	Age > 40 a						1399 ± 93$^{\#}$	1685 ± 84	
		CKD	11	Mean eGFR 51 ± 15	Yes	eGFR	2-h fasting	TRIG	IR SE EPI	1530 ± 99$^{\#}$	1726 ± 78	T_2*, DWI, PC, ASL

The given T_1 relaxation times of the cortex and medulla are mean ± SD in ms. Patient studies are highlighted in grey.

3D, three-dimensional; ^{99m}Tc-DTPA, ^{99m}Tc-diethylene triamine pentaacetic acid; a, year; bFFE, balanced fast field echo; BOLD, blood oxygen level dependant; BH, breath hold; CKD, chronic kidney disease; CO_2, carbon dioxide; DWI, diffusion-weighted imaging; EPI, echo-planar imaging; e/mGFR, estimated or measured glomerular filtration rate (in mL/min/1.73 m^2); GE, gradient echo; FFE, fast field echo; FSE, fast spin echo; FLASH, fast low angle shot; FB, free breathing; HASTE, half Fourier acquisition single shot turbo spin echo; LuTx, lung transplantation; MDRD, modification of diet in renal disease; ME, multi-echo; MS, multishot; PC, phase contrast; SE, spin-echo; SS, single shot; T, Tesla; T_1, spin–lattice relaxation time; T_2, spin–spin relaxation time; T_2*, apparent transverse relaxation time; T_1w, T_1 weighted; TRIG, triggered MRI acquisition with regards to breathing motion; trueFISP, true fast imaging with steady-state precession; TSE, turbo spin echo.

[a]Recalculated and corrected values.

Other symbols refer to the statistical significance within the associated study:

$^{\diamond}P < 0.0001$; $^{\dagger,\ddagger,\blacktriangledown,\blacktriangleleft,\blacktriangleright}P < 0.001$; $^{\int}P < 0.005$; $^{\S}P < 0.008$; $^{\#}P < 0.01$; $^{\circ}P < 0.01$; $^{\bullet}P = 0.01$; $^{\blacksquare}P = 0.03$; $^{\square}P = 0.047$; $^{*}P < 0.05$.

dependent (BOLD) MRI, associated changes are reviewed by Pruijm *et al.* [30].

To our knowledge, modulations of renal T_1 values during the inhalation of pure oxygen (O_2) and carbogen (5% carbon dioxide mixed with 95% O_2) were only observed in healthy volunteers. In 2002, Jones *et al.* [21] reported a significant decrease in cortical T_1 values during O_2 inhalation at 1.5T. These findings were confirmed in 2007 and 2009 with an even more pronounced reduction in cortical T_1 values following the inhalation of O_2 and carbogen [23, 24]. In these studies, the lack of a renal hydration protocol [except in O'Connor *et al.* [24]], the free breathing acquisition, the VFA method and dyspnoea during the carbogen inhalation (leading to increased breathing motion), as well as the temporal and spatial acquisition constraints, can be considered as important limitations [23, 24].

The first 3T study was carried out by Ding *et al.* [27] when healthy subjects were evaluated during exposure to normoxia and O_2. Thereafter a multiparametric renal MRI study evaluated five healthy volunteers who underwent a hyperoxia challenge (~80% O_2); again cortical T_1 values decreased, but unlike previous publications, no statistical significance was observed [18].

These studies show that cortical T_1 is sensitive to oxygenation level changes. However, the contribution of vasoconstriction and vasodilatation as well as perfusion changes during O_2 and carbogen inhalation, as well as the evaluation of renal oxygen delivery (ischaemia), were never directly assessed, which could have caused the reported ambiguous findings [18, 27]. Final conclusions regarding medullary T_1 modulations are currently not possible. Last but not least, it has not been clarified yet as to what extent alterations in T_1 reflect tissue and/or blood oxygenation. These questions remain a target for future evaluations.

Clinical studies

Renal transplants—early qualitative and semi-quantitative MRI studies. Imaging of renal transplants in the iliac fossae is less confounded by breathing motion, which enabled renal MRI evaluations in the 1980s [31]. Early qualitative and/or semi-quantitative renal MRI studies revealed a reduced T_1 CMD in acute allograft rejection (AAR), and even diminished T_1 CMD in chronic allograft rejection (CAR) [15, 31–34]. However, acute tubular necrosis (ATN) could not be sufficiently differentiated from AAR [32, 34–36], and even diminished T_1 CMD was reversible in some cases of ATN and AAR [36]. Thus scrutiny of the reduced T_1 CMD linked both oedema and fibrosis to prolonged T_1 values, which partially explains the low specificity of these renal transplant evaluations [37].

Another interesting finding on renal transplant observation was the clearly preserved T_1 CMD during an acute decline in renal function under cyclosporine therapy, which was linked to cyclosporine nephrotoxicity (CN) [32, 34]. However, three successive studies presented ambiguous outcomes [33, 37, 38]. Thereafter, no further research efforts were made, so no final conclusion can be made.

All these envisioned early MRI studies on renal transplants applied field strengths <1.5T, which today are not frequently in clinical use. However, in contrast to recent MRI evaluations, all of these studies applied histological validation. A low specificity was observed due to different acquisition settings (e.g. vendors and protocols), low reproducibility of the two-point method to calculate T_1 [31] and lack of a standardized patient preparation (e.g. hydration protocol) [14, 15]. In addition, loss of T_1 CMD was reversible after clinical improvement in some cases of ATN and ARR, which could have decreased the specificity further [36]. Therefore recommendations could not advocate qualitative and/or semi-quantitative MRI evaluations over ultrasound and scintigraphy [34].

Renal transplants—quantitative MRI studies. T_1 measurements on renal transplants at 1.5T were presented by Huang *et al.* [19] in 2011, when renal transplants and native kidneys with unknown underlying renal disease confirmed the trend of higher cortical and medullary T_1 values in renal transplants. They also achieved a high short-term *in vivo* repeatability (~±10%). In addition, strong correlations were observed between estimated glomerualr filtration rate (eGFR) and cortical T_1 in both groups (native cortex: $r = -0.83$, $P = 0.0001$; transplant cortex: $r = -0.80$, $P = 0.0017$), but medullary T_1 values only significantly correlated with eGFR in the transplant group ($r = -0.94$, $P < 0.0001$) [19].

The second quantitative T_1 assessment of renal transplant was presented by Friedli *et al.* [29]. A total of 29 patients underwent a multiparametric MRI approach at 3T, including a validation against histological samples. With regard to T_1, only T_1 CMD showed a moderate correlation with renal interstitial fibrosis ($R^2 = 0.29$, $P < 0.001$) and eGFR ($R^2 = 0.22$, $P < 0.05$). No correlation was established between T_1 values and cellular inflammation [29]).

In 2018, renal T_1 was evaluated in 49 renal transplant patients, 52 patients after lung transplantation (LuTx; native kidneys) and 14 healthy volunteers [26]. Their aim was to assess acute kidney injury (AKI) after LuTx (reported incidence ~60%), and after a 3- and 6-month follow-up. T_1 CMD was significantly decreased and mean cortical and medullary T_1 were significantly higher in renal transplants compared with healthy volunteers and the LuTx group ($P < 0.001$). However, T_1 CMD was also reduced in the LuTx group compared with volunteers ($P < 0.05$), which was linked to the incidence of AKI after LuTx. All patients and healthy volunteers were further grouped according to Kidney Disease Outcomes Quality Initiative (KDOQI) stages. Remarkable were the significantly lower cortical T_1 values in subjects with eGFR $\geq$60 mL/min/1.73 m^2 as compared with <60 mL/min/1.73 m^2 and that cortical T_1 negatively correlated ($r = -0.642$, $P < 0.001$) and T_1 CMD positively correlated ($r = 0.542$, $P < 0.001$) with eGFR for all participants. In contrast, medullary T_1 showed only a weak correlation with eGFR ($r = -0.341$, $P < 0.001$). During the 3- and 6-month follow-up, cortical T_1 and T_1 CMD exhibited a significant correlation with eGFR ($P < 0.001$ and < 0.01, respectively) in the LuTx and renal transplantation groups [26].

In summary, we identified only three quantitative T_1 studies on renal allografts at 1.5 and 3T. In contrast to early qualitative and semi-quantitative MRI studies, only one quantitative study applied a histological validation, in which it was shown that

Table 2. Quantitative T_2 studies at 1.5 and 3T

Author	Year	Subject	Sample size	Group	*In vivo* repeatability	GFR	Hydration	Respiratory compensation	Sequence	Cortex	Medulla	Other modalities
1.5T												
de Bazelaire *et al.* [11]	2004	Healthy	4	—	No	Not measured	None	BH	SE T_2 prep	87 ± 4	85 ± 11	T_1
Zhang *et al.* [45]	2011	Healthy	4	Day 1	Yes	Not measured	None	BH	2D ME TSE	112†	137†	T_2*
			4	Day 2						112†	143†	
Mathys *et al.* [46]	2011	Healthy	6	—	No	TUC	2-h fasting	FB	ME SE	125 ± 7$^{\#,\circ}$	–	T_2*
		Renal allograft	6	GFR >40	No	TUC	2-h fasting	FB	ME SE	147 ± 13$^{\#}$	–	T_2*
		Renal allograft	9	GFR <40						150 ± 20°		
3T												
de Bazelaire *et al.* [11]	2004	Healthy	6	—	No	Not measured	None	BH	SE T2 prep	76 ± 7	81 ± 8	T_1
Li *et al.* [12]	2015	Healthy	5	—	No	Not measured	None	BH	CPMG T2 prep	121 ± 5	138 ± 7	T_1
Franke *et al.* [47]	2017	Healthy	3	—	No	Not measured	None	—	ME GE SE	132 ± 6$^{\#,\blacktriangleleft,\blacktriangledown}$		–
		ADPKD	3	TKV <300 mL	No	Not measured	None	—	ME GE SE	417 ± 65$^{\#,*}$		–
			3	TKV 300–400 mL						592 ± 231$^{\blacktriangleleft}$		
			3	TKV >400 mL						669 ± 170 $^{*\blacktriangledown}$		

The given T_2 relaxation times of the cortex and medulla are mean ± SD in ms. Patient studies are highlighted in grey.

2D, two dimensional; BH, breath-hold; FB, free breathing; GE, gradient echo; ME, multi-echo; prep, preparation; T, Tesla; T_1, spin–lattice relaxation time; T_2, spin–spin relaxation time; T_2*, apparent transverse relaxation time; T_1w, T_1 weighted; TKV, total kidney volume; TUC, timed urine collection; TSE, turbo spin echo.

†Recalculated: reported values in mean ± SD: R_2 day 1: 8.9 ± 0.6s^{-1} (cortex) and 7.3 ± 0.7s^{-1} (medulla); day 2: 8.9 ± 0.6s^{-1} (cortex) and 7.0 ± 0.7s^{-1} (medulla).

Other symbols refer to the statistical significance within the associated study:

$^{\blacktriangledown,\blacktriangleleft}P < 0.001$; $^{\#}P < 0.01$; $^{\circ}P < 0.01$; $^{*}P < 0.05$.

state-of-the-art T_1 measurements, i.e. T_1 CMD, could be used to assess renal interstitial fibrosis in allografts [29]. Another important finding was that T_1 values were sensitive to presumable AKI alterations in the context of post-LuTx [26]. However, the specificity of renal MRR regarding AAR, CAR, ATN or drug-induced toxicity was not further assessed or improved. Furthermore, these studies show that T_1 mapping has the potential to estimate renal function.

Non-invasive assessment of renal function. The first quantitative T_1 measurements on patients at 1.5T were published in 2007 [22]. A small and unbalanced group was primarily enrolled for the evaluation of a renal artery stenosis: one patient with CKD and hypertension and nine patients with hypertension alone. A loose hydration protocol was applied before the MRI acquisition, and afterwards all patients underwent a ^{99m}Tc-diethylene triamine pentaacetic acid renography to measure the single-kidney GFR (SKGFR). A significant correlation was depicted only between cortical T_1 values and the SKGFR ($r = -0.5$, $P = 0.03$) [22].

In 2015 the association between cortical T_1, renal perfusion (from arterial spin labeling (ASL); see also Odudu *et al.* [39]) and eGFR in patients with chronic heart failure (HF) and control subjects with different levels of renal impairment was evaluated [25]. Renal perfusion was similar in chronic HF patients with and without renal impairment, but cortical T_1 showed a significant correlation with eGFR ($r = -0.41$, $P = 0.015$), which reflects the potential to assess CKD. Chronic HF patients had significantly higher cortical T_1 compared with all control subjects, and chronic HF patients with renal impairment had significantly higher cortical T_1 compared with chronic HF patients without renal impairment [25].

After the ASL reproducibility study of Gillis *et al.* in 2014 [20], a follow-up study evaluated renal perfusion and cortical T_1 in healthy volunteers and CKD patients with different a etiologies at 3T. Significantly higher cortical T_1 values were found in CKD patients and a correlation between cortical T_1 and eGFR was observed ($r = -0.58$, $P < 0.001$) [28].

One year later a multiparametric renal MRI study assessed T_1 in healthy subjects and CKD patients with various renal diseases after a short fasting period (>2 h) at 3T [18]. Compared with volunteers, CKD showed significantly higher cortical T_1, and T_1 CMD was reduced ($P < 0.01$). They achieved an interscan coefficient of variation of <2.9% and high intraclass correlation for the cortex and medulla (0.848 and 0.997, respectively, using spin-echo echo-planar imaging) [18].

As previously envisioned also, three renal transplant studies assessed the correlation of T_1 values and the renal function at 1.5 and 3T (see above) [19, 26, 29].

In summary, the envisioned studies show that the degree of renal impairment correlates moderately to strongly with cortical T_1 and T_1 CMD in CKD with various renal diseases [18, 22, 28], renal transplants [19, 26, 29], and chronic HF patients [25]. These findings are also in line with some qualitative assessments in the 1990s [40, 41], but not with all [42], due to the fact that renal T_1 values are modulated by many confounders, such as the degree of fibrosis [29], comorbidities (e.g. liver cirrhosis) [43, 44], the acquisition protocol (e.g. breathing motion) and fastening and hydration level [14], which all together seem to be responsible for the accomplished correlations in the envisioned quantitative studies at 1.5 and 3T. To our knowledge, only one study correlated renal T_1 values with measured GFR [22]. It should be noted that adequate patient preparation (e.g. hydration protocol, medication intake), patient selection in the context of comorbidities and acquisition protocols (e.g. triggered breath-hold) together with reference measurement of the renal function can improve T_1 renal function correlations, which advocates for further research in this field.

RENAL T_2 MAPPING

Reference values and physiological modulations

In healthy subjects, medullary T_2 is consistently longer than cortical T_2. As previously envisioned, Hricak *et al.* [14] evaluated the effect of fasting and hydration and showed that T_2 CMD decreased during hydration (i.e. forced diuresis), but these findings were never re-evaluated. Additional variation can also be found due to the increase in B_0 from 1.5 and 3T, which is accompanied by a general decrease in T_2, and by the fact that different MRI acquisitions and breathing strategies report unequal values. But for healthy subjects a high day-to-day repeatability was shown by a multi-echo spin-echo method with a mean variability of <4% for both cortex and medulla at 1.5T [45].

Closely linked to T_2 is T_2', which is thought to reflect tissue oxygenation [45, 46]. For measurement of T_2', both T_2 and T_2^* are required. T_2^*, i.e. renal BOLD MRI, is discussed by Pruijm *et al.* in this issue [30].

These variations have to be considered when comparing different studies (Table 2).

Clinical studies

In the 1980s renal transplants were evaluated regarding T_2, and MRI was shown to be useful to identify fluid collections in necrotic transplant, perinephric lymphoceles and haematoma [31].

To our knowledge, the first quantitative clinical, i.e. renal transplant, study on T_2 values at 1.5Tesla (T) was reported in 2011. One of two T_2 acquisition protocols identified a significant increase in cortical T_2 in 15 renal transplants compared with 6 healthy subjects. However, no significant difference was observed with regards to the allograft function [46].

In 2017, whole kidney T_2 values in animals with juvenile cystic kidneys and nine autosomal dominant polycystic kidney disease (ADPKD) patients were reported. A strong significant increase in T_2 values was seen in early-stage ADPKD patients compared with healthy volunteers. Based solely on T_2 values, early-stage ADPKD patients with a kidney volume <300 mL could be distinguished from healthy volunteers, which was not possible based on total kidney volume (TKV) [47].

In summary, human *in vivo* measurements of renal T_2 are relatively scarce. Therefore no final conclusion can be made regarding renal function estimation or renal transplant assessments. Nevertheless, interesting findings were obtained, which clearly advocate for future research. Early-stage ADPKD

patients could benefit from the T_2 evaluations and the potentially improved assessment of early-disease progression compared with TKV [47]. This might be of special interest in the evaluation of novel therapeutic agents such as tolvaptan. The assessment of AKI in the context of ischaemia reperfusion injury, e.g. induced kidney damage during renal allograft surgery, also seems to be a potential application for T_2, as *in vivo* measurements were shown to be feasible [46]. Animal studies have shown that T_2 is sensitive to ischaemia–reperfusion injury [48, 49]. During initial ischaemia, T_2 decreases, probably due to deoxygenation, followed by an increase during reperfusion [50]. In the longer term, an elevation of T_2 that is more pronounced in the medulla compared with the cortex has been found [51, 52], which was attributed to consecutive inflammation and oedema (T_2 increase) [50–52]. Human studies are necessary to determine whether the T_2 changes following AKI can predict the recovery of renal function.

DISCUSSION

In recent decades, quantitative renal T_1 and T_2 mapping have been shown not only to be feasible, but also to provide non-invasive valuable information regarding renal structure and function in healthy, AKI, CKD, renal transplant and ADPKD patients at 1.5 and 3T (Tables 1 and 2).

Renal T_1 has been shown to be modulated by hydration and, in particular, cortical T_1 was sensitive to oxygenation. T_1 CMD is a potential candidate biomarker to assess AAR, CAR, ATN, CN, fibrosis and renal function. Renal T_2 was measured in only a few studies but showed the potential to evaluate renal transplants and to improve the diagnosis and progression of early-stage ADPKD.

However, the variation in T_1 and T_2 values is large, mainly due to the great diversity of the MRR methods applied, but also due to physiological (e.g. water balance management during fasting and forced diuresis) and pathological alterations (e.g. fibrosis) of the renal parenchyma. In virtually all renal diseases, renal function and microstructure are altered together, and this review on T_1 and T_2 unveiled the high sensitivity towards each of these processes as well as the complicated interpretation of the acquired data due to the low specificity.

In conclusion, currently available data suggest that the full potential of renal T_1 and T_2 mapping has not yet been tapped and adequate patient selection, with regard to comorbidities, alongside technical and physiological standardization, will significantly increase the specificity of renal MRR. On route towards renal T_1 or T_2 mapping as a biomarker it will be necessary to validate renal MRR against widely accepted reference measurements (e.g. nuclear medicine evaluations) as well as against histological findings, when possible. Last but not least, the integration of different quantitative renal MRI data into a multiparametric approach will likely enable us to gain the best insight into renal pathophysiology. The COST Action PARENCHIMA (www.renalmri.org) is working on standardization of multiparametric renal MRI techniques to tackle these challenges.

SUPPLEMENTARY DATA

Supplementary data are available at ndt online.

ACKNOWLEDGEMENTS

This article is based upon work from the COST Action Magnetic Resonance Imaging Biomarkers for Chronic Kidney Disease (PARENCHIMA), funded by COST (European Cooperation in Science and Technology). www.cost.eu. For additional information, please visit PARENCHIMA project website: www.renalmri.org.

FUNDING

M.W. was supported by the Austrian Science Fund (FWF; project P28867). A.d.B. was supported by an Alexandre Suerman scholarship for MD/PhD students at the University Medical Center Utrecht, Utrecht, The Netherlands. K.S. was supported by the Biomarker Enterprise to Attack Diabetic Kidney Disease project funded by the Innovative Medicines Initiative 2 Joint Undertaking under grant agreement 115974. This joint undertaking received support from the European Union's Horizon 2020 research and innovation programme and European Federation of Pharmaceutical Industries and Associations. P.B. was supported by Deutsche Forschungsgemeinschaft (BO 3755/6-1, SFB/TRR57, SFB/TRR219) and by the German Ministry of Education and Research (BMBF Consortium STOP-FSGS number 01GM1518A). N.P.J. was supported by the Liaison Committee for Education, Research and Innovation in Central Norway (grant number 90065000).

CONFLICT OF INTEREST STATEMENT

None declared.

REFERENCES

1. Moser E, Stadlbauer A, Windischberger C *et al.* Magnetic resonance imaging methodology. *Eur J Nucl Med Mol Imaging* 2009; 36(Suppl 1): S30–S41
2. Bloch F, Hansen WW, Packard M. Nuclear Induction. *Phys Rev* 1946; 69: 127
3. Rinck PA. *Magnetic Resonance in Medicine: A Critical Introduction.* Norderstedt, Germany: – Books on Demand, 2018
4. Cheng H-LM, Wright GA. Rapid high-resolution T_1 mapping by variable flip angles: accurate and precise measurements in the presence of radiofrequency field inhomogeneity. *Magn Reson Med* 2006; 55: 566–574
5. Wang HZ, Riederer SJ, Lee JN. Optimizing the precision in T1 relaxation estimation using limited flip angles. *Magn Reson Med* 1987; 5: 399–416
6. Look DC, Locker DR. Time saving in measurement of NMR and EPR relaxation times. *Rev Sci Instrum* 1970; 41: 250–251
7. Messroghli DR, Radjenovic A, Kozerke S *et al.* Modified Look-Locker inversion recovery (MOLLI) for high-resolution T1 mapping of the heart. *Magn Reson Med* 2004; 52: 141–146
8. Messroghli DR, Greiser A, Fröhlich M *et al.* Optimization and validation of a fully-integrated pulse sequence for modified look-locker inversion-recovery (MOLLI) T1 mapping of the heart. *J Magn Reson Imaging* 2007; 26: 1081–1086
9. Brown RW, Cheng Y-CN, Mark Haacke E *et al. Magnetic Resonance Imaging: Physical Principles and Sequence Design.* Canada; Hoboken, NJ: John Wiley & Sons, 2014
10. Kellman P, Aletras AH, Mancini C *et al.* T2-prepared SSFP improves diagnostic confidence in edema imaging in acute myocardial infarction compared to turbo spin echo. *Magn Reson Med* 2007; 57: 891–897
11. de Bazelaire CMJ, Duhamel GD, Rofsky NM *et al.* MR imaging relaxation times of abdominal and pelvic tissues measured in vivo at 3.0 T: preliminary results. *Radiology* 2004; 230: 652–659
12. Li X, Bolan PJ, Ugurbil K *et al.* Measuring renal tissue relaxation times at 7 T. *NMR Biomed* 2015; 28: 63–69

13. Messroghli DR, Moon JC, Ferreira VM *et al.* Clinical recommendations for cardiovascular magnetic resonance mapping of T1, T2, T2* and extracellular volume: a consensus statement by the Society for Cardiovascular Magnetic Resonance (SCMR) endorsed by the European Association for Cardiovascular Imaging (EACVI). *J Cardiovasc Magn Reson* 2017; 19: 75
14. Hricak H, Crooks L, Sheldon P *et al.* Nuclear magnetic resonance imaging of the kidney. *Radiology* 1983; 146: 425–432
15. Marotti M, Hricak H, Terrier F *et al.* MR in renal disease: importance of cortical-medullary distinction. *Magn Reson Med* 1987; 5: 160–172
16. Blüml S, Schad LR, Stepanow B *et al.* Spin-lattice relaxation time measurement by means of a TurboFLASH technique. *Magn Reson Med* 1993; 30: 289–295
17. Chen Y, Lee GR, Aandal G *et al.* Rapid volumetric T1 mapping of the abdomen using three-dimensional through-time spiral GRAPPA. *Magn Reson Med* 2016; 75: 1457–1465
18. Cox EF, Buchanan CE, Bradley CR *et al.* Multiparametric renal magnetic resonance imaging: validation, interventions, and alterations in chronic kidney disease. *Front Physiol* 2017; 8: 696
19. Huang Y, Sadowski EA, Artz NS *et al.* Measurement and comparison of T1 relaxation times in native and transplanted kidney cortex and medulla. *J Magn Reson Imaging* 2011; 33: 1241–1247
20. Gillis KA, McComb C, Foster JE *et al.* Inter-study reproducibility of arterial spin labelling magnetic resonance imaging for measurement of renal perfusion in healthy volunteers at 3 Tesla. *BMC Nephrol* 2014; 15: 23
21. Jones RA, Ries M, Moonen CTW *et al.* Imaging the changes in renal T1 induced by the inhalation of pure oxygen: a feasibility study. *Magn Reson Med* 2002; 47: 728–735
22. Lee VS, Kaur M, Bokacheva L *et al.* What causes diminished corticomedullary differentiation in renal insufficiency? *J Magn Reson Imaging* 2007; 25: 790–795
23. O'Connor JPB, Jackson A, Buonaccorsi GA *et al.* Organ-specific effects of oxygen and carbogen gas inhalation on tissue longitudinal relaxation times. *Magn Reson Med* 2007; 58: 490–496
24. O'Connor JPB, Naish JH, Jackson A *et al.* Comparison of normal tissue R_1 and R_2 modulation by oxygen and carbogen. *Magn Reson Med* 2009; 61: 75–83
25. Breidthardt T, Cox EF, Squire I *et al.* The pathophysiology of the chronic cardiorenal syndrome: a magnetic resonance imaging study. *Eur Radiol* 2015; 25: 1684–1691
26. Peperhove M, Vo Chieu VD, Jang M-S *et al.* Assessment of acute kidney injury with T1 mapping MRI following solid organ transplantation. *Eur Radiol* 2018; 28: 44–50
27. Ding Y, Mason RP, McColl RW *et al.* Simultaneous measurement of tissue oxygen level-dependent (TOLD) and blood oxygenation level-dependent (BOLD) effects in abdominal tissue oxygenation level studies. *J Magn Reson Imaging* 2013; 38: 1230–1236
28. Gillis KA, McComb C, Patel RK *et al.* Non-contrast renal magnetic resonance imaging to assess perfusion and corticomedullary differentiation in health and chronic kidney disease. *Nephron* 2016; 133: 183–192
29. Friedli I, Crowe LA, Berchtold L *et al.* New magnetic resonance imaging index for renal fibrosis assessment: a comparison between diffusion-weighted imaging and T1 mapping with histological validation. *Sci Rep* 2016; 6: 30088
30. Pruijm M, Mendichovszky IA, Liss P *et al.* Renal blood oxygenation level-dependent magnetic resonance imaging to measure renal tissue oxygenation: a statement paper and systematic review. *Nephrol Dial Transplant* 2018; 33 (Suppl 2): ii22–ii28
31. Geisinger MA, Risius B, Jordan ML *et al.* Magnetic resonance imaging of renal transplants. *AJR Am J Roentgenol* 1984; 143: 1229–1234
32. Hricak H, Terrier F, Demas BE. Renal allografts: evaluation by MR imaging. *Radiology* 1986; 159: 435–441
33. Baumgartner BR, Nelson RC, Ball TI *et al.* MR imaging of renal transplants. *AJR Am J Roentgenol* 1986; 147: 949–953
34. Hricak H, Terrier F, Marotti M *et al.* Posttransplant renal rejection: comparison of quantitative scintigraphy, US, and MR imaging. *Radiology* 1987; 162: 685–688
35. Steinberg HV, Nelson RC, Murphy FB *et al.* Renal allograft rejection: evaluation by Doppler US and MR imaging. *Radiology* 1987; 162: 337–342
36. Liou JT, Lee JK, Heiken JP *et al.* Renal transplants: can acute rejection and acute tubular necrosis be differentiated with MR imaging? *Radiology* 1991; 179: 61–65
37. Winsett MZ, Amparo EG, Fawcett HD *et al.* Renal transplant dysfunction: MR evaluation. *AJR Am J Roentgenol* 1988; 150: 319–323
38. Mitchell DG, Roza AM, Spritzer CE *et al.* Acute renal allograft rejection: difficulty in diagnosis of histologically mild cases by MR imaging. *J Comput Assist Tomogr* 1987; 11: 655–663
39. Odudu A, Nery F, Harteveld AA *et al.* Arterial spin labelling MRI to measure renal perfusion: a systematic review and statement paper. *Nephrol Dial Transplant* 2018; 33 (Suppl 2): ii15–ii21
40. Semelka RC, Chew W, Hricak H *et al.* Fat-saturation MR imaging of the upper abdomen. *AJR Am J Roentgenol* 1990; 155: 1111–1116
41. Semelka RC, Corrigan K, Ascher SM *et al.* Renal corticomedullary differentiation: observation in patients with differing serum creatinine levels. *Radiology* 1994; 190: 149–152
42. Kettritz U, Semelka RC, Brown ED *et al.* MR findings in diffuse renal parenchymal disease. *J Magn Reson Imaging* 1996; 6: 136–144
43. Lee KS, Muñoz A, Báez AB *et al.* Corticomedullary differentiation on T1-weighted MRI: comparison between cirrhotic and noncirrhotic patients. *J Magn Reson Imaging* 2012; 35: 644–649
44. Yamada F, Amano Y, Hidaka F *et al.* Pseudonormal corticomedullary differentiation of the kidney assessed on T1-weighted imaging for chronic kidney disease patients with cirrhosis. *Magn Reson Med Sci* 2015; 14: 165–171
45. Zhang JL, Storey PH, Rusinek H *et al.* Reproducibility of R2* and R2 measurements in human kidneys. *Proc Int Soc Magn Reson Med* 2011; 19: 2954
46. Mathys C, Blondin D, Wittsack H-J *et al.* T_2' imaging of native kidneys and renal allografts - a feasibility study. *Rofo* 2011; 183: 112–119
47. Franke M, Baeßler B, Vechtel J *et al.* Magnetic resonance T2 mapping and diffusion-weighted imaging for early detection of cystogenesis and response to therapy in a mouse model of polycystic kidney disease. *Kidney Int* 2017; 92: 1544–1554
48. Yuasa Y, Kundel HL. Magnetic resonance imaging following unilateral occlusion of the renal circulation in rabbits. *Radiology* 1985; 154: 151–156
49. Thickman D, Kundel H, Biery D. Magnetic resonance evaluation of hydronephrosis in the dog. *Radiology* 1984; 152: 113–116
50. Pohlmann A, Hentschel J, Fechner M *et al.* High temporal resolution parametric MRI monitoring of the initial ischemia/reperfusion phase in experimental acute kidney injury. *PLoS One* 2013; 8: e57411
51. Ko S-F, Yip H-K, Zhen Y-Y *et al.* Severe bilateral ischemic-reperfusion renal injury: hyperacute and acute changes in apparent diffusion coefficient, T1, and T2 mapping with immunohistochemical correlations. *Sci Rep* 2017; 7: 1725
52. Hueper K, Rong S, Gutberlet M *et al.* T2 relaxation time and apparent diffusion coefficient for noninvasive assessment of renal pathology after acute kidney injury in mice: comparison with histopathology. *Invest Radiol* 2013; 48: 834–842

Received: 30.4.2018; Editorial decision: 29.5.2018